

Effects of Knee Simulator Loading and Alignment Variability on Predicted Implant Mechanics: A Probabilistic Study

Peter J. Laz,¹ Saikat Pal,¹ Aaron Fields,¹ Anthony J. Petrella,² Paul J. Rullkoetter¹

¹University of Denver, Department of Engineering, 2390 South York, Denver, Colorado 80208 USA

²DePuy, a Johnson & Johnson Company, 700 Orthopaedic Drive, Warsaw, Indiana 46581

Received 20 December 2005; accepted 24 May 2006

Published online 26 September 2006 in Wiley InterScience (www.interscience.wiley.com). DOI 10.1002/jor.20254

ABSTRACT: Inherent variability in total knee arthroplasty loading and alignment, present in vivo and in simulator testing, may ultimately influence polyethylene tibial insert wear and long-term performance. The effect of this variability was quantified on implant kinematics and contact mechanics during simulated gait loading conditions using semi-constrained and unconstrained fixed bearing, cruciate retaining implants. A probabilistic finite element model of the Stanmore knee wear simulator was utilized to estimate the envelope of anterior–posterior (AP) and internal–external (IE) position and contact pressure and to evaluate the variability in corresponding ranges of motion (ROM). Variability levels were represented by standard deviations of up to 10% of the maximum value for load inputs and 0.25 mm and 0.5° for component alignment inputs. Model predictions compared well with experimental simulator results for the semi-constrained implant, with predicted positional envelopes of up to 1.8 mm (AP) and 3.4° (IE) for the semi-constrained and up to 2.6 mm (AP) and 3.7° (IE) for the unconstrained implant at the variability levels evaluated. ROM varied by up to 22%, while peak contact pressure variations averaged less than 2 MPa for both designs. For each implant, loading variability was more influential during the swing phase of gait, while alignment variability affected kinematics more during stance. The relative rank of sensitivities showed differences between the two designs, providing insight into critical parameters affecting kinematics and contact characteristics. © 2006 Orthopaedic Research Society. Published by Wiley Periodicals, Inc. *J Orthop Res* 24:2212–2221, 2006

Keywords: knee simulator; variability; kinematics; sensitivity; wear

INTRODUCTION

Potentially significant variability in total knee arthroplasty (TKA) loading and alignment exists in vivo, as well as in experimental knee simulator tests. Variability has been reported both in joint loading^{1–3} and resulting kinematics.⁴ Joint loading is naturally impacted by body weight (BW); however, even when body weight is normalized, joint loading exhibits considerable variability. In a gait study on natural knees, Taylor and colleagues¹ determined peak tibiofemoral joint contact forces between 2.97 and 3.33 BW in four patients using a musculoskeletal lower limb model. For a BW of 666 N, the peak force would vary by 240 N. This study also showed that the joint force magnitude and variability are larger during stair climbing than during gait. Variability has also been quantified in association with component placement,^{5–8} as malalignment remains an under-

lying cause for revision surgery. In a study of 673 TKAs, Mahaluxmivala and colleagues⁵ reported standard deviations of 2.3° for insert varus–valgus (VV) angle, 3.5° for insert tilt, and 3.9° for the femoral component flexion angle. In a study of 10 cadaveric specimens, Siston and colleagues⁶ measured a standard deviation of 6.5° for femoral internal–external (IE) rotational alignment when evaluating five different reference axes. In a review article, Zihlmann and coworkers⁷ noted that malalignment occurred in approximately 10% to 30% of patients with observed femoral IE alignment ranging from 6° internal to 8° external rotation.

Similarly, variability in loading and kinematics⁹ and in resulting wear rates^{10,11} is commonly observed in simulator testing. Force controlled wear simulators^{9,12} aim to reproduce knee joint loading to evaluate kinematics and wear of implant designs. Component wear is related to interface contact pressures and relative motions,^{13–15} and changes in kinematics have been directly related to wear rate in in vitro studies.^{10,16} McEwen and colleagues estimated that kinematics with a 50%

Correspondence to: Peter J. Laz (Telephone: 303-871-3614; Fax: 303-871-4450; E-mail: plaz@du.edu)

© 2006 Orthopaedic Research Society. Published by Wiley Periodicals, Inc.

reduction in sliding distance from 0–10 mm (anterior-posterior (AP) translation and $\pm 5^\circ$ (IE rotation) to 0–5 mm and $\pm 2.5^\circ$, resulted in a fourfold reduction in wear rate.¹⁰ Similarly, Kawanabe and colleagues¹⁶ observed increased (6- to 11-fold) wear rates when including $\pm 5^\circ$ of IE rotation and 0 to 12 mm of AP translation. In both simulator and in vivo cases, the potential variability in implant kinematics and contact mechanics likely influence wear and ultimately long-term performance.

The aims of the present study were to develop a probabilistic finite element (FE) model of the Stanmore knee wear simulator capable of including loading, alignment, and environmental variability and to assess the impact of this variability on predicted tibiofemoral mechanics by determining the potential envelope of joint kinematics and contact mechanics of a semi-constrained and an unconstrained TKA during gait loading. The effects of only alignment and environmental variability have been studied previously for a single implant.¹⁷ The ranges of motion (ROM), because they relate to sliding distance, provide an indication of wear variability, while the size of the performance envelopes provide insight into design robustness. In addition, the sensitivity of the implant relative position and ROM to the study variables was assessed to identify the critical loading, alignment, and environmental parameters affecting each design.

In the longer term, the techniques developed in this study can be applied to in vivo levels of variability. The prediction of a performance envelope rather than a single deterministic result provides information about not only the level of performance, but also the likelihood of a specific level of performance. While studies^{18–20} have applied optimization to implant design for specific criteria, few studies^{21,22} have evaluated design robustness by considering variability in the inputs (e.g., loading, bone properties, and alignment). Robustness is a measure of how consistently a specific implant design performs when considering patient variation, such as loading and constraint variability, and small malalignments in implant position. In the current study, the size of the performance envelope is explored as a measure of robustness with the approach developed providing a platform for initial assessments of component robustness. The determination of optimal envelope sizes for performance measures, including kinematics, contact mechanics, wear, load transfer, and joint strength, is especially difficult, as holistic consideration of these multiple and potentially competing measures is required.

METHODS

Finite Element Model

Explicit FE models of the fixed bearing, cruciate retaining TKA with semi-constrained and unconstrained tibial inserts were developed in Abaqus/Explicit (Abaqus, Inc., Providence, RI) to represent the mechanical environment of the Stanmore knee simulator.^{9,12} The semi-constrained geometry had a single sagittal radius, while the unconstrained implant was flat centrally with a posterior lip. The meshes and boundary conditions of the FE model (Fig. 1) were based on previous studies by Halloran and colleagues.^{23,24} The femoral component (same for each insert) was modeled using 20874 three-dimensional (3D) surface elements, while eight-noded hexahedral elements (8351 for semi-constrained, 10,878 for unconstrained) were used to represent the tibial components.

The applied loading represented simulated gait in the Stanmore knee simulator.^{12,25} A femoral flexion angle and compressive load were applied to the femoral component, while an AP force and IE torque were applied to the tibial component. The tibial component was constrained in the inferior–superior (IS), flexion–extension (FE), and VV degrees of freedom and was free in the medial–lateral (ML) degree of freedom. The femoral component was constrained in AP, ML, and IE, and unconstrained in the VV degree of freedom. The compressive load profile was offset toward the medial condyle to reproduce the experimental 60% to 40% load split. Springs representing soft tissue constraint on the knee simulator were also included in the model.^{12,23}

Mesh convergence was verified previously.²³ For computational efficiency, the components were represented as rigid bodies with a previously verified pressure–overclosure relationship that was optimized for each implant geometry and mesh.²⁴ Halloran and colleagues demonstrated excellent correlation between fully deformable and rigid body analyses under the same loading conditions while reducing computation time from ~6 h to ~6 min.²⁴

Probabilistic Model

The probabilistic analyses were performed by interfacing Nesus (probabilistic modeling software, Southwest Research Institute, San Antonio, TX) and Abaqus. The probabilistic analysis included variability in 16 normally distributed parameters, including 4 loading, 4 translational and 4 rotational alignment, and 4 experimental set-up parameters (Fig. 1, Table 1). Converged results were obtained using the more efficient Advanced Mean Value (AMV) method^{26,27} and the Monte Carlo method.

Variability in the loading profiles was quantified from published data⁹ by determining a range for each of the loading profiles at 100 temporal locations throughout the gait cycle. While the variability was presented for 6 different designs, the same loading condition was desired for each implant and it was therefore assumed

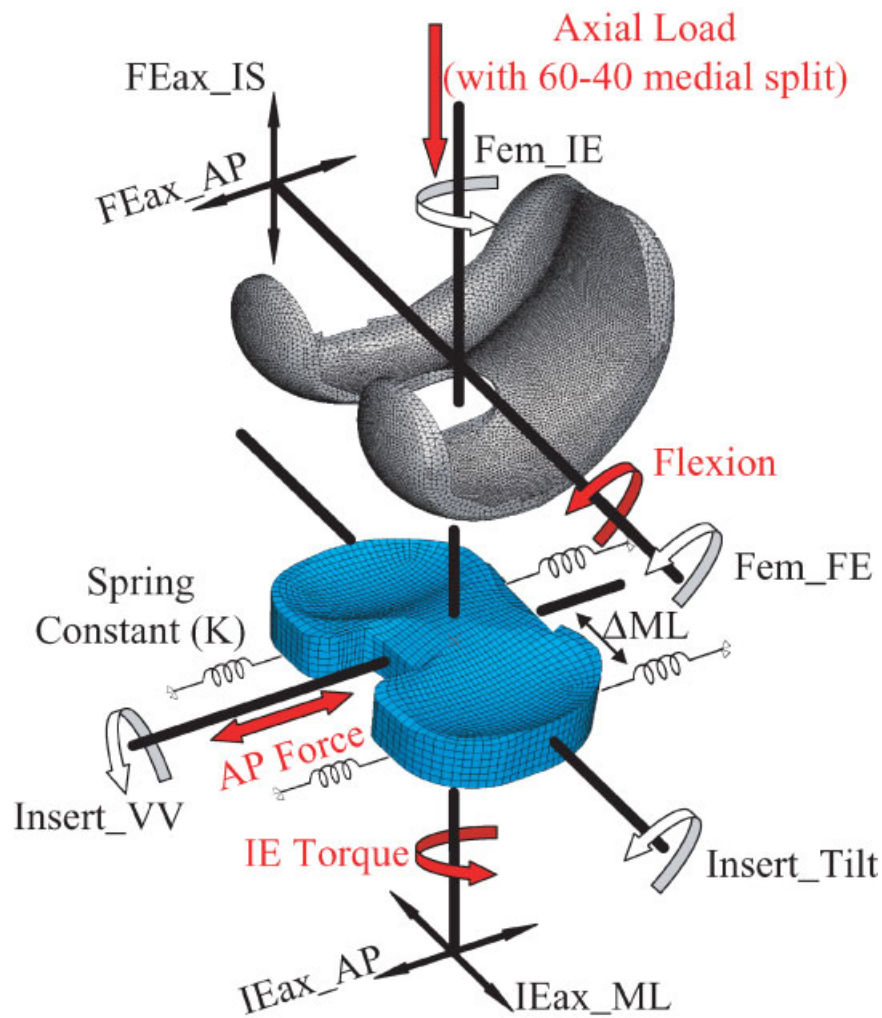


Figure 1. Finite element model of TKR illustrating the boundary conditions and study parameters (not shown: ML load split and μ).

Table 1. Study Parameters with Mean and Standard Deviation

Parameter	Description	Mean	Standard Deviation
Flexion	Femoral flexion	Profile from ISO standard ²⁵	0.11°
Load	Compressive axial force	Profile from ISO standard ²⁵	18.75 N
AP force	AP force	Profile from ISO standard ²⁵	up to 20.63 N ^a
IE torque	IE torque	Profile from ISO standard ²⁵	up to 0.37 Nm ^a
FEax_AP	AP position of femoral FE axis	0 mm	0.25 mm
FEax_IS	IS position of femoral FE axis	25.4 mm	0.25 mm
IEax_AP	AP position of tibial IE axis	7.62 mm	0.25 mm
IEax_ML	ML position of tibial IE axis	0 mm	0.25 mm
Fem_FE	Initial femoral FE rotation	0°	0.5°
Fem_IE	Initial femoral IE rotation	0°	0.5°
Insert_tilt	Tilt (FE rotation) of the tibial insert	0°	0.5°
Insert_VV	VV position of the tibial insert	0°	0.5°
AML	ML position of spring fixation	28.7 mm	0.5 mm
K	Spring constant	5.21 N/mm	0.09 N/mm
ML_split	ML load split (60%–40%)	60%	2.5%
μ	Coefficient of friction	0.04	0.01

^aStandard deviations varied throughout the gait cycle.

that a similar level of variability could be applied to a single implant design. The standard deviation for each parameter and location was estimated by assuming that the experimental range represented $\pm 2\sigma$. Using the experimental variability, the standard deviations were nearly constant for the compressive load cycle (18.7 N) and the femoral flexion angle (0.11°), while the standard deviations varied for AP force (up to 20.6 N) and IE torque (up to 0.37 Nm). The standard deviation as a percentage of the maximum value in the cycle⁹ was 0.8% for compressive load, 0.2% for flexion, 9.1% for AP force, and 4.9% for IE torque. For each loading parameter in a single gait analysis, one perturbation (standard normal variate) was determined and then mapped throughout the cycle using the standard deviations at each temporal location. This technique accounted for the different variability levels observed throughout the gait cycle in the AP force and IE torque.⁹

The translational and rotational alignment parameters represented variability in component alignment in the experiment (Fig. 1, Table 1). The alignment parameters included: the AP and IS position of the femoral flexion axis, the AP and ML position of the tibial IE rotation axis, the initial flexion and IE rotation of the femoral component, and the tilt and VV position of the insert. Mean position of both implants was based on the neutral position of the semi-constrained implant from the simulator test. The variability in the component alignment parameters was not readily available; it was selected conservatively at a level which could be achieved with careful experimental practice. The standard deviations were estimated as 0.25 mm and 0.5° for the translational and rotational parameters, respectively. This level of variability implies that 95% of the data are within ± 2 standard deviations (0.5 mm and 1.0°). The experimental parameters were the load split, the ML position of spring fixation, the soft tissue spring constant (K), and the coefficient of friction (μ). For each parameter, the means were determined from the actual set-up, while standard deviations were conservatively estimated from the experiment. The variability in coefficient of friction during experimental testing is not well understood, but was approximated to capture the range reported in the literature.^{28–30}

The model predicted the resulting envelope (1–99 percentiles) for three performance measures: AP and IE position of the tibial insert and contact pressure (CP). To evaluate whether the predicted kinematic envelope was primarily a shift in the relative position of the implant or an actual change in the magnitude of the relative motion, the ROM for AP and IE positions was also computed as the difference between minimum and maximum positions over the gait cycle.

Sensitivity factors for the AP and IE position data, peak contact pressure, and AP and IE ROM were also determined. The sensitivities are relative measures of how much the performance metric was affected by variability in each input parameter. The calculation of sensitivity factors in the AMV method is complex. Briefly, sensitivities were based on the unit vector specifying the

most probable point in the transformed standard normal variate space. As a result, the sum of the squares of the sensitivity factors for all of the variables unity. A more detailed description can be found in Haldar and Mahadevan.²⁷ To provide straightforward ranking of the variables, the absolute averages of the sensitivities were calculated over the desired region of the gait cycle. For AP and IE position and contact pressure, sensitivity was separated into stance (0%–60% gait) and swing phase (60%–100% gait), while a single value was reported for the scalar ROM data.

RESULTS

The AP and IE kinematic results for the semi-constrained design compared well with experimental data for the implant²³ obtained from force controlled gait simulation in the knee simulator^{9,12} (Fig. 2). The predicted envelopes of AP and IE position showed considerable kinematic variability and were similar in size for both implants (Figs. 2 and 3). The semi-constrained implant position varied by up to 1.8 mm and 3.4° , with averages of 1.5 mm and 2.2° , while the unconstrained position (Fig. 3) varied by up to 2.6 mm and 3.7° , with averages of 1.7 mm and 2.4° . Experimental data for the unconstrained implant were unavailable for comparison. In addition, the envelope sizes for contact pressure (Fig. 4) averaged 1.5 MPa and 2.0 MPa with maximums of 2.8 MPa and 4.1 MPa for the semi-constrained and unconstrained implants, respectively. For comparison, the peak contact pressures in the semi-constrained and unconstrained implants were approximately 18 and 24 MPa, respectively.

The ROM results (Table 2) highlight the relative motion during the gait cycle. Average ROM was larger in AP and IE for the unconstrained implant, a result of its lesser conformity. The differences between the 1% and 99% bounds of ROM were 0.73 mm (AP) and 1.7° (IE) for the semi-constrained implant and 1.36 mm (AP) and 1.46° (IE) for the unconstrained implant. In both cases, the variability in ROM for AP and IE was potentially significant, comprising 13% to 20% (semi-constrained) or 10% to 22% (unconstrained) of the average ranges.

Critical sensitivity factors for AP and IE position were similar for the two designs; however, differences were present in the relative rank (Fig. 5). For the semi-constrained implant, insert tilt variability (sensitivity factor, 0.88) was the most important for affecting AP position during the stance phase, with lesser contributions from the friction (0.24), AP force (0.23), and femoral flexion alignment (0.20)

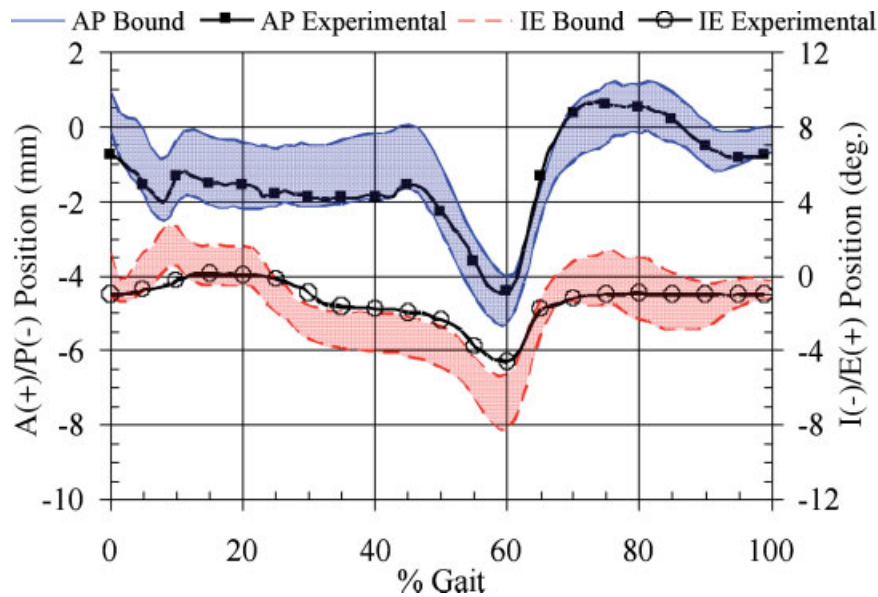


Figure 2. Experimental AP and IE positions with model-predicted envelopes (1%–99%) as a function of gait cycle for the semi-constrained design.

variability. The same parameters were identified for the unconstrained implant, with an increased importance of AP force variability (0.45). In contrast to the stance phase, swing phase positional variability was most affected by AP force variability, with contributions from insert tilt, compressive load, and friction. Swing phase varia-

bility in IE position was dominated by the IE torque variability (>0.90) for both implants; however, differences were seen in the stance phase. The IE position for the semi-constrained implant was primarily affected by the femoral IE rotational alignment (0.85), while the unconstrained implant had more balanced contributions from the IE

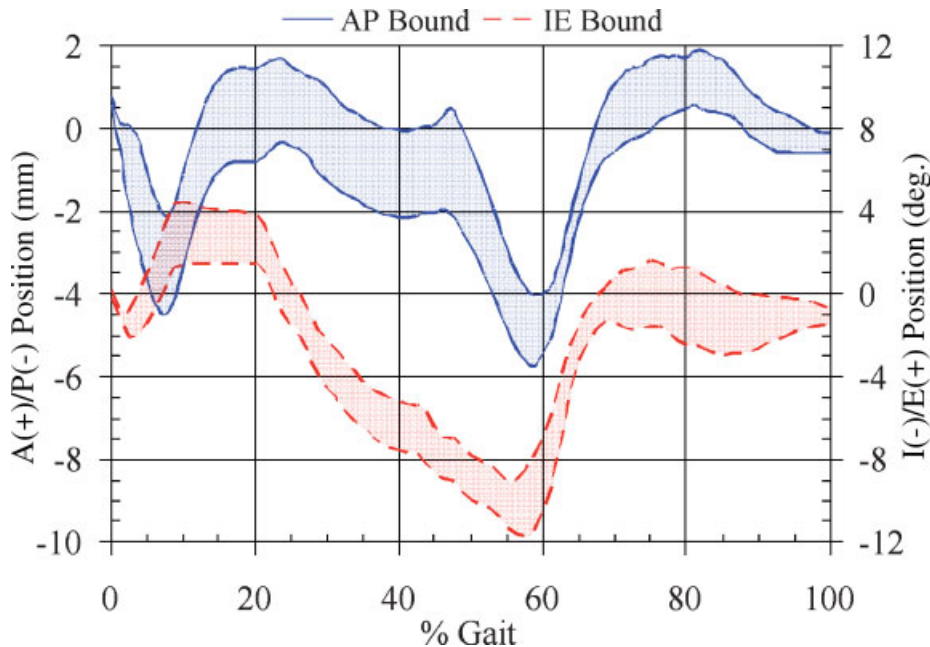


Figure 3. Model-predicted envelopes (1%–99%) for AP and IE positions as a function of gait cycle for the unconstrained design. Experimental data were not available for comparison.

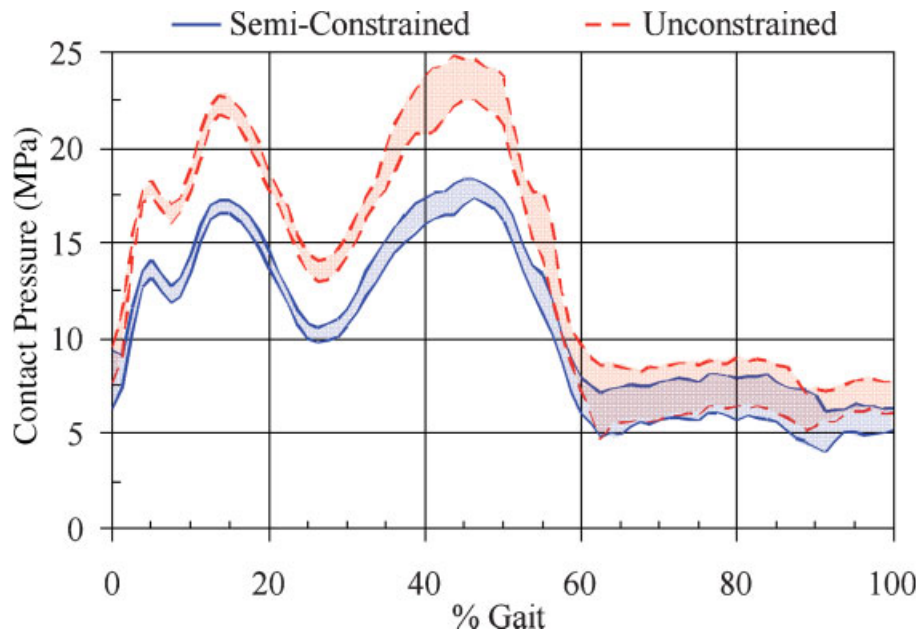


Figure 4. Model-predicted envelopes (1%–99%) for contact pressure as a function of gait cycle for the semi-constrained and unconstrained implants.

torque, femoral IE rotational alignment, and friction variability (Fig. 5). Both implants exhibited similar sensitivity factors affecting contact pressure; during stance, the load split (~ 0.60), the compressive load, insert VV, and friction were all important, while compressive load (~ 0.90) was the dominant parameter during swing.

For AP ROM, differences were again present in the relative rank of critical parameters for the two designs (Figure 6). Compressive load was more important for the semi-constrained implant, while friction and insert tilt were more important for the unconstrained design.

DISCUSSION

The probabilistic model developed in this study incorporated variability present in loading, alignment, and experimental set-up and predicted the variability in performance of kinematics, contact

pressure, and ROM for the two designs under simulated gait conditions. In comparison with previous work, including the loading variability increased the size of the AP and IE position envelopes primarily during the swing phase; the stance phase positional variability was comparable.¹⁷ The performance envelope size provides an indication of the robustness of a design to input variability. Based on the similarly sized performance envelopes (Figs. 2–4), the robustness of the two designs was effectively equivalent for the loading and variability studied. Because of its lesser conformity, intuition may lead one to believe that the unconstrained implant would be more robust and less affected by variable perturbations. While the mean positions and contact pressures of the two implants were different, their envelope sizes were quite similar. This somewhat surprising result can be explained when considering the sensitivity factors, which indicate that in

Table 2. Average and Bounds (1% and 99%) of Kinematic Ranges of Motion (ROM) for the Semi-Constrained and Unconstrained Implants

Performance metric	Semi-Constrained Implant			Unconstrained Implant		
	Average	Minimum	Maximum	Average	Minimum	Maximum
AP ROM (mm)	5.22	5.08	5.81	6.11	5.43	6.80
IE ROM ($^{\circ}$)	8.48	7.71	9.41	13.29	12.63	14.09

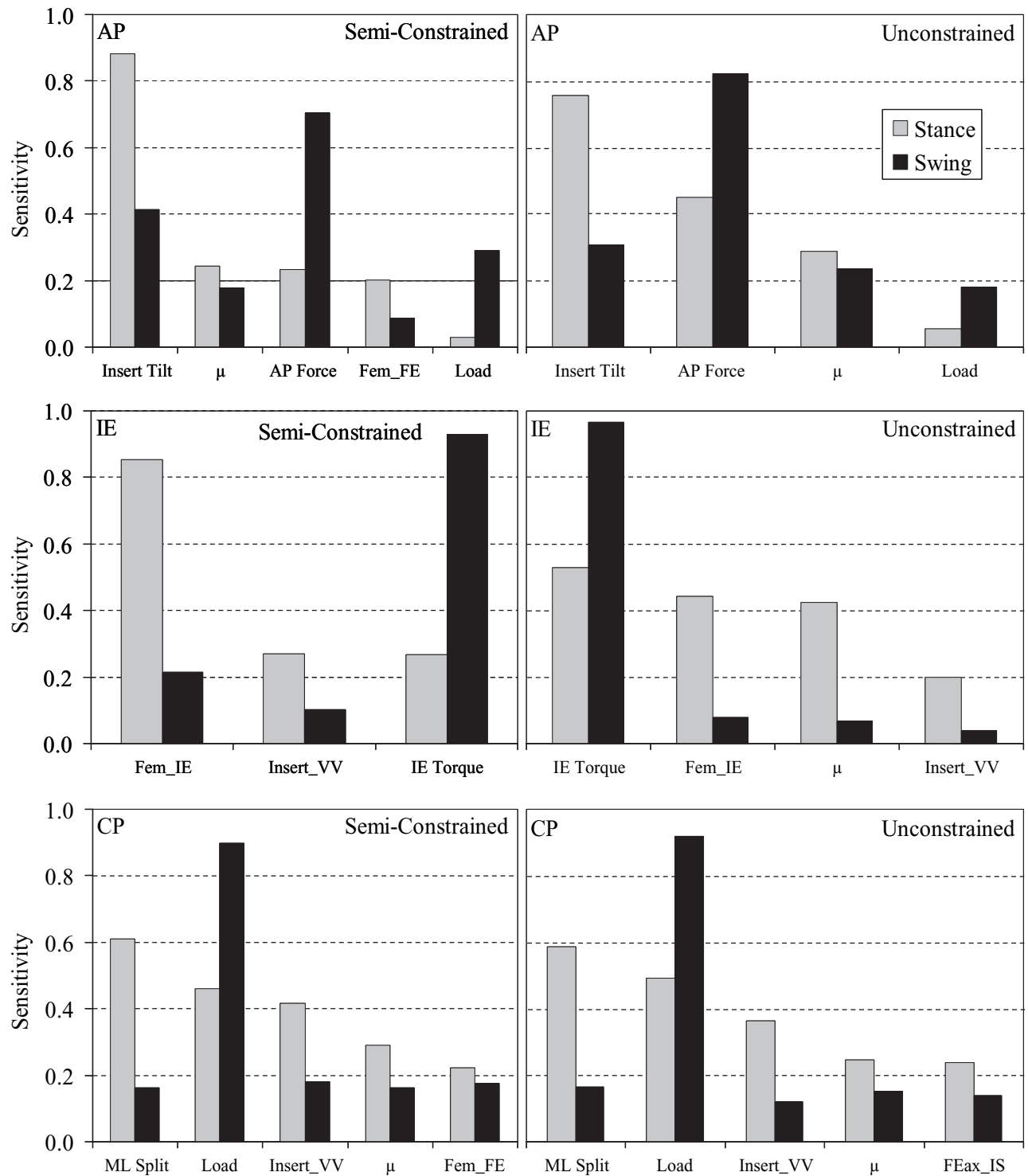


Figure 5. Stance and swing phase sensitivity of AP and IE position and contact pressure (CP) for the most important variables for the semi-constrained and unconstrained implants. Data presented in decreasing order of importance during the stance phase.

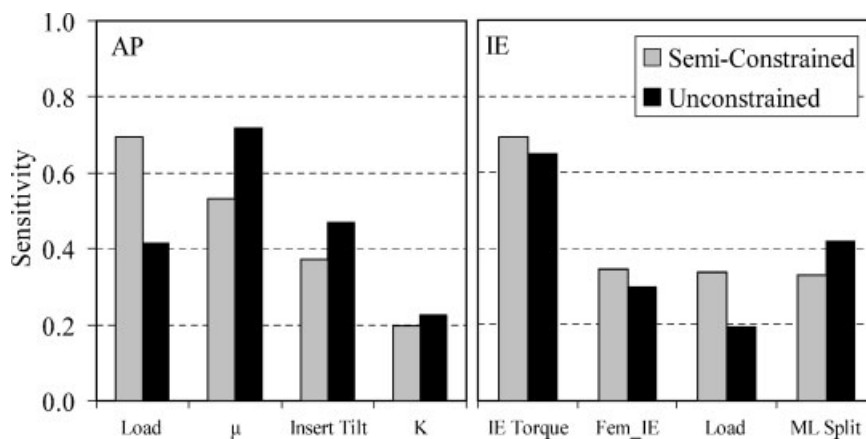


Figure 6. Sensitivity of AP (left) and IE (right) range of motion for the four most important variables.

comparison to the semi-constrained implant the performance of the unconstrained implant was generally more affected by the loading and frictional variability than the alignment variability.

The probabilistic approach provides a platform for making assessments of variability in performance, which provide useful insights into the robustness of a design. Robustness is a relative measure dependent on the input level of variability. Consideration of both performance envelopes and sensitivity factors can be incorporated in the design evaluation process and in the development of surgical procedures to lead hopefully to more consistent performance outcomes.

Because the ROM data influences sliding distance, the variability in the kinematic data, representing up to 20% for the semi-constrained implant and 22% for the unconstrained implant, has the potential to impact wear. McEwen and colleagues found a fourfold reduction in wear rate with a 50% reduction in sliding distance.¹⁰ While the average ROM values in this study are smaller for AP translation and comparable for IE rotation, the nominally 20% ROM variability observed will affect wear rate. Variability in predicted contact pressure was smaller, averaging less than 2 MPa for both implants, which implies that simulator wear variability under these testing conditions is likely due more to kinematic variability.

The sensitivity factors demonstrated the critical parameters for the stance and swing phase position for each implant and differentiated the two implants with their relative rank. Insert tilt, friction, AP force, and femoral flexion alignment were most important to both implants during the stance phase, with the unconstrained implant more

dependent on the AP force variability, as expected by the decreased conformity compared with the semi-constrained implant. The force/torque variability (compressive load, AP force, IE torque) was most important during swing. Stance phase IE position sensitivity was different for the implants; the more conforming semi-constrained was most dependent on alignment variables (femoral IE alignment), while the unconstrained was also affected by friction and torque. The critical sensitivity factors were also different for ROM; the AP range for the unconstrained insert was more dependent on friction and insert tilt, whereas the more conforming semi-constrained was most dependent on compressive load. Commonly varied surgical parameters were identified as important to the predicted position and ROM, including insert tilt^{31,32} and femoral IE alignment.^{7,33} Given the potential range of surgical alignments, substantial resulting performance variability may occur.

While the variability levels utilized in this study were selected to represent a carefully controlled experiment, they were substantially smaller than variability measured in vivo. Joint loading variability included standard deviations up to 20.6 N and 0.37 Nm, which are considerably smaller than the variability in peak tibiofemoral joint contact forces of up to 240 N.¹ The standard deviations for component alignment were 0.25 mm and 0.5°. Considerable component alignment variability, both unintentional and from differing surgical philosophy, has been quantified in the literature. Mahaluxmivala and colleagues⁵ measured standard deviations of up to 4° for rotational alignment, while Zihlmann and coworkers⁷ reported rotational alignment ranging from 6°

internal rotation to 8° external rotation. Substantial variability also may be found with surgical choices for important variables, such as implanting the tibial component perpendicular to the mechanical axis or reproducing a natural level of posterior tibial slope.³⁴

Substantial variability was predicted in performance when modeling simulated gait loading conditions with relatively small standard deviations. Because of the greater variability observed in loading and alignment in vivo, even larger kinematic envelopes and greater differences in ROM are expected. The use of computer assisted surgical systems has reduced variability in component alignment over manual techniques.^{35,36} The probabilistic approach, if coupled with a more realistic representation of the in vivo loading conditions, can be used to evaluate potential benefits associated with reduced alignment variability using computer assisted techniques. A quantitative understanding of the performance variability and key variables affecting it can also be useful when evaluating TKA designs for a population of patients.

Several limitations in this analysis may impact the presented results. The standard deviation levels for the loading parameters were based on the spread in data between six established implants.⁹ By selecting a constant perturbation level for each loading profile in each probabilistic trial, the loading variability was appropriately captured; however, higher order shifting and scaling affects through the gait cycle were not considered. Although a carefully controlled in vitro environment is desired to provide experimental validation of model predictions, simplification of the soft-tissue restraint (springs all within transverse plane) limits the significance of VV implant positioning, which is important in vivo. Because this study is based on a simulator, the contributions of joint loading and alignment on kinematics and contact mechanics can be isolated. In reality, patient geometry and component placement are directly linked to joint loading. Further enhancement of the FE model representation has the potential to link loading and geometry to provide a more accurate assessment of in vivo conditions.

In conclusion, this study has quantified the effects of variability in loading, component alignment, and environment on simulated TKA joint mechanics. At the variability levels evaluated, the predicted envelopes and ROMs have the potential to impact component performance, including wear. While these findings are based on experimental wear simulator conditions, the approach developed

can be used to evaluate the performance and robustness of implant designs when subject to the greater levels of variability in surgical alignment and loading conditions observed in vivo.

REFERENCES

1. Taylor WR, Heller MO, Bergmann G, et al. 2004. Tibio-femoral loading during human gait and stair climbing. *J Orthop Res* 22:625–632.
2. Nagura T, Dyrby CO, Alexander EJ, et al. 2002. Mechanical loads at the knee joint during deep flexion. *J Orthop Res* 20:881–886.
3. Baliunas AJ, Hurwitz DE, Ryals AB, et al. 2002. Increased knee joint loads during walking are present in subjects with knee osteoarthritis. *Osteoarthritis Cartilage* 10: 573–579.
4. Dyrby CO, Andriacchi TP. 2004. Secondary motions of the knee during weight bearing and non-weight bearing activities. *J Orthop Res* 22:794–800.
5. Mahalaxmivala J, Bankes MJK, Nicolai P, et al. 2001. The effect of surgeon experience on component positioning in 673 press fit condylar posterior cruciate-sacrificing total knee arthroplasties. *J Arthroplasty* 16:635–640.
6. Siston RA, Patel JJ, Goodman SB, et al. 2005. The variability of femoral rotational alignment in total knee arthroplasty. *J Bone Joint Surg Am* 87:2276–2280.
7. Zihlmann MS, Stacoff A, Romero J, et al. 2005. Biomechanical background and clinical observations of rotational malalignment in TKR: literature and consequences. *Clin Biomech* 20:661–668.
8. Brys DA, Lombardi AV, Mallory TH, et al. 1991. A comparison of intramedullary and extramedullary alignment systems for tibial component placement in total knee arthroplasty. *Clin Orthop* 263:175–179.
9. DesJardins JD, Walker PS, Haider H, et al. 2000. The use of a force-controlled dynamic knee simulator to quantify the mechanical performance of total knee replacement designs during functional activity. *J Biomech* 33:1231–1242.
10. McEwen HMJ, Barnett PI, Bell CJ, et al. 2005. The influence of design, materials and kinematics on the in vitro wear of total knee replacements. *J Biomech* 38: 357–365.
11. Muratoglu OK, Bragdon CR, Jasty M, et al. 2004. Knee-Simulator testing of conventional and cross-linked polyethylene tibial inserts. *J Arthroplasty* 19:887–897.
12. Walker PS, Blunn GW, Broome DR, et al. 1997. A knee simulating machine for performance evaluation of total knee replacements. *J Biomech* 30:83–89.
13. Blunn GW, Walker PS, Joshi A, et al. 1991. The dominance of cyclic sliding in producing wear in total knee replacements. *Clin Orthop* 273:253–260.
14. Schwenke T, Borgstede LL, Schneider E, et al. 2005. The influence of slip velocity on wear of total knee arthroplasty. *Wear* 259:926–932.
15. Wimmer MA, Andriacchi TP. 1997. Tractive forces during rolling motion of the knee: implications for wear in total knee replacement. *J Biomech* 30:131–137.
16. Kawanabe K, Clarke IC, Tamura J, et al. 2001. Effects of A–P translation and rotation on the wear of UHMWPE in a total knee joint simulator. *J Biomed Mat Res* 54:400–406.

17. Laz PJ, Pal S, Halloran JP, et al. 2005. Probabilistic finite element prediction of knee wear simulator mechanics. *J Biomech* 39:2303–2310.
18. Huiskies R, Boeklagen R. 1989. Mathematical shape optimization of hip prosthesis design. *J Biomech* 22:763–804.
19. Nicoletta DP, Thacker BH, Katoozian H, et al. 2005. The effect of three-dimensional shape optimization on the probabilistic response of a cemented femoral hip prosthesis. *J Biomech* 39:1265–1278.
20. Kowalzyk P. 2001. Design Optimization of cementless femoral hip prostheses using finite element analysis. *J Biomech Eng* 123:396–402.
21. Chang PB, Williams BJ, Bawa Bahalla KS, et al. 2001. Design and analysis of robust total joint replacements: Finite element model experiments with environmental variables. *J Biomech Eng* 123:239–246.
22. Viceconti M, Brusi G, Pancanti A, et al. 2005. Primary stability of an anatomical cementless hip stem: a statistical analysis. *J Biomech* 39:1169–1179.
23. Halloran JP, Petrella AJ, Rullkoetter PJ. 2005. Explicit finite element modeling of total knee replacement mechanics. *J Biomech* 38:323–331.
24. Halloran JP, Easley SK, Petrella AJ, et al. 2005. Comparison of deformable and elastic foundation finite element simulations for predicting knee replacement mechanics. *J Biomech Eng* 127:813–818.
25. International Standards Organization. 2000. ISO Standard 14243-2. Wear of total knee-joint prostheses, Part 2: methods of measurement. Geneva, Switzerland: International Standards Organization.
26. Wu YT, Millwater HR, Cruse TA. 1990. Advanced probabilistic structural analysis method for implicit performance functions. *AIAA J* 28:1663–1669.
27. Haldar A, Mahadevan S. 2000. Probability, reliability and statistical methods in engineering design. New York: Wiley.
28. Fisher J, Dowson D. 1991. Tribology of total artificial joints. *Proc Inst Mech Eng* 205:73.
29. Sathasivam S, Walker PS. 1997. A computer model with surface friction for the prediction of total knee kinematics. *J Biomech* 30:177–184.
30. Godest AC, Beaugonin M, Haug E, et al. 2002. Simulation of a knee joint replacement during gait cycle using explicit finite element analysis. *J Biomech* 35:267–275.
31. Walker PS, Garg A. 1991. Range of motion in total knee arthroplasty. *Clin Orthop* 262:227.
32. Dorr LD, Boiardo RA. 1986. Technical considerations in total knee arthroplasty. *Clin Orthop* 205:5–11.
33. Sodha S, Kim J, McGuire KJ, et al. 2004. Lateral retinacular release as a function of femoral component rotation in total knee arthroplasty. *J Arthroplasty* 19:459–463.
34. Catani F, Fantozzi S, Ensini A, et al. 2006. Influence of tibial component posterior slope on in vivo knee kinematics in fixed-bearing total knee arthroplasty. *J Orthop Res* 24:581–587.
35. Kim SJ, MacDonald M, Hernandez J, et al. 2005. Computer assisted navigation in total knee arthroplasty: improved coronal alignment. *J Arthroplasty* 20:123–131.
36. Sparmann M, Wolke B, Czupalla H, et al. 2003. Positioning of total knee arthroplasty with and without navigation support. *J Bone Joint Surg Br* 85:830–835.